On the Fenton degradation mechanism. The role of oxalic acid

Yamila Alegría[a], Fernando Liendo,[b] and Oswaldo Núñez[a]*

[a] Laboratorio de Química Ambiental, Departamento de Procesos y Sistemas. Universidad Simón Bolívar. Apartado postal 89000. Caracas, Venezuela. [b]Gerencia de Ecología y Ambiente. PDVSA Intevep. Apartado postal 76343. Caracas, 1070A, Venezuela
E-mail: onunez@usb.ve

Dedicated to Professors Roberto A. Rossi on his 60th anniversary and Edmundo A. Ruveda on his 70th anniversary

(received 19 Aug 03; accepted 12 Nov 03; published on the web 04 Dec 03)

Abstract

Kinetics of Fenton (Fe(II) + H_2O_2) *p*-nitrophenol degradation reveal that the measured pseudo first-order rate constant is given by the expression: $k_{obs} = kK [H_2O_2]/ (1 + K[H_2O_2])$, where K= 20.3 x 10^2 M^{-1} is the equilibrium constant of formation of the complex Fe(II)-$(H_2O_2)_n$ and k= 1.5 x 10^{-2} s^{-1} is the first order rate constant of degradation of the complex to yield Fe (III), $OH^{\cdot}$ and OH^-. When oxalic acid is added, the complex Fe(III)-oxalic acid-H_2O_2 is formed producing a highly oxidized Fe(IV) species as the primary oxidant agent.

Keywords: Fenton, *p*-nitrophenol, pseudo first-order, Fe(III)-oxalic acid-complex

Introduction

The Fenton reagent[1] (Fe(II)/H_2O_2) constitutes one of the so called Advanced Oxidation Process (AOP's) that has been used for the decontamination of organic pollutants from water. This process application in water treatment is widely recognized. For instance, we have treated[2], at the laboratory scale, typical oil industry effluents from production and petrochemical activities as well as artificial water samples containing: *m*-cresol, 2-chlorophenol, methyl tert-butylether and reformulated gasoline. The Fenton reagent has been also used to degrade organic chlorides, pesticides, monocyclic aromatics as well to reduce the COD (chemical oxygen demand) of municipal waters[3-9]. It also has been used in the decontamination of soils[10].

It has been proposed[11-14] that the reaction mechanism involves formation of the hydroxyl radical in a rate limiting step (Eq.1) with further diffusion-controlled rate radical attack to the organic substrate.

$$Fe^{+2} + H_2O_2 \rightarrow Fe^{+3} + OH^- + OH^{\cdot} \quad (1)$$

It has been also proposed[14] that a highly oxidized intermediate is formed previous to the hydroxyl radical formation (Eq. 2).

$$Fe^{+2} + H_2O_2 \rightarrow (FeOH)^{+3} = Fe^{+3} + OH^{\cdot} \quad (2)$$

Besides hydroxyl radical, as the primary oxidant, a higher valence iron (Eq.3) or iron-oxygen complex[15,16,17] has been proposed. In the last case, intramolecular oxidation-reduction is presented as evidence of Fe (IV) intermediate.

$$Fe^{+2} + H_2O_2 \rightarrow FeO^{2+} + H_2O \quad (3)$$

In this paper we focus on the detailed mechanism of the hydroxyl radical formation and explore practical conditions that accelerate and retard the reaction. Kinetic evidence for a pre-equilibrium between free reactants and its complex previous to the rate limiting hydroxyl radical formation is presented. Reaction is improved when oxalic acid is added to the reaction. A new path (besides the hydroxyl radical one) is then contributing to the oxidation. Important evidence in favor of the participation of a highly oxidized iron species are given by monitoring COD (chemical oxygen demand) during reaction progress.

Results and Discussion

1. Experiments changing [H_2O_2]

In Table 1, pseudo first-order rate constants, at different [H_2O_2] ratios, obtained from plots of ln [*p*-nitrophenol] vs. t are shown. In Figure 1, the obtained $k_{obs.}$ values are plotted vs. [H_2O_2].

Table 1. Pseudo first-order rate constants at different [H_2O_2]. T: 25 ^oC; pH = 2.8. $k_{obs.}$ deviation values obtained from triplicates

Ratio (*p*-Nitrophenol:H_2O_2: Fe(II))	[H_2O_2] x 10^3 (M)	k_{obs} x 10^3 (s^{-1})
1:5:1	0.5	8.1 ± 0.3
1:8:1	0.8	8.7 ± 0.4
1:14:1	1.4	12.4 ± 0.1
1:17:1	1.7	12.5 ±0.6
1:20.1	2	12.0 ± 0.3

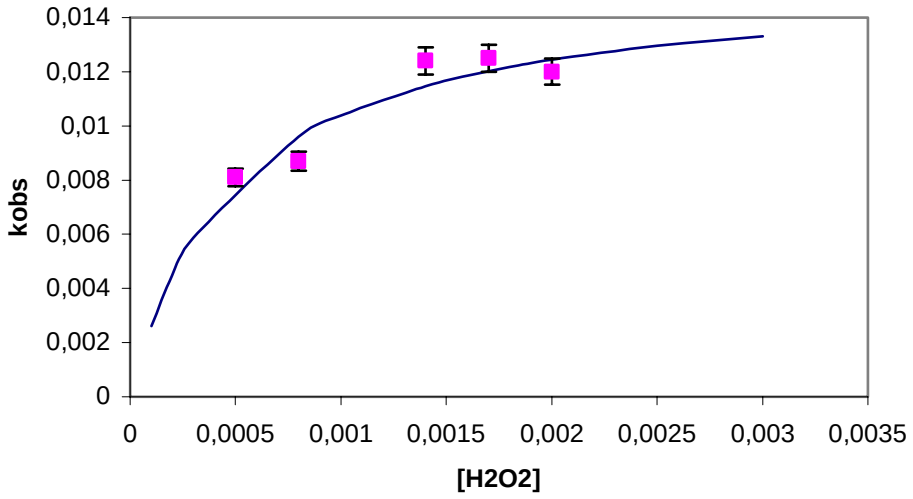

Figure 1. Plot of pseudo-first order rate constants (k_{obs}) vs. [H_2O_2]. T= 25 ^oC. pH = 2.8. Experimental points and error (4%) bars from triplicates are shown. Continuous line corresponds to Eq. 5 theoretical values, with k= 0.015 s^{-1} and K = 2034 M^{-1}. k and K values were obtained from a plot of 1/kobs vs. 1/[H_2O_2] (Figure 2).

The k_{obs}. vs. [H_2O_2] profile, corresponds to a pseudo first-order mechanism in which an equilibrium prior to the rate limiting step is established as shown in Eq. 4. Eq. 5, shows the corresponding rate law.

$$Fe^{+2} + n\ H_2O_2 \underset{}{\overset{K}{\rightleftharpoons}} Fe\text{-}(H_2O_2)_n \xrightarrow{k} Fe^{+3} - (H_2O_2)_{n-1} + HO^- + HO^{\bullet} \qquad (4)$$

where,
$$k_{obs} = \frac{K\,k\,[H_2O_2]}{1 + K\,[H_2O_2]} \qquad (5)$$

In Figure 2, a plot of 1/kobs vs. 1/[H_2O_2] is shown. From the intercept, a k= 0.0155 s^{-1} is directly obtained and from the slope (slope = 1/kK), K = 2034 M^{-1} is found. These values were used to simulate, using Eq. 5, the predicted kobs at different [H_2O_2] (Figure 1, continuous line). According to Eq. 5 when 1 > K[H_2O_2], kobs = kK [H_2O_2]; from where a kK= 31.5 $s^{-1}M^{-1}$ is obtained.

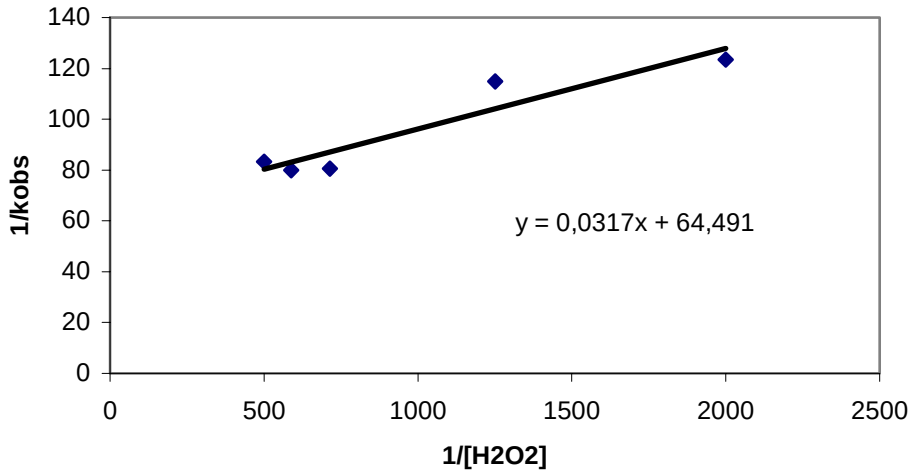

Figure 2. $1/k_{obs}$ vs. $1/[H_2O_2]$. From the intercept = 64.49 = 1/k, k = 0.0155 s^{-1} is obtained and from the slope = 0.031 = 1/kK, K = 2034 M^{-1} is found.

Using a Fe(II): H_2O_2 (1:14) ratio and following the appearance of the Fe(III) UV band at 220 nm, a pseudo first-order rate constant of 2.4 (± 0.3) x 10^{-2} s^{-1}, similar to the value obtained from Figure 1 is found. When Fe(III) is used instead of Fe(II) with initial ratios: *p*-nitrophenol:H_2O_2:Fe(III) = 1:5:1, following the UV band at 330 nm, an induction period of ca. 450 s is observed followed by pseudo first-order decay with a slope of 7.6(± 0.6) x 10^{-3} s^{-1}. This value is also similar to the one obtained from Figure 1 indicating that after the induction period Fe (II) is regenerated[18] to produce OH as proposed in Eq. 4.

2. Experiments varying pH

Kinetics, following *p*-nitrophenol absorbance (330 nm, at acid pH or 400 nm, at neutral or basic pH) vs. time at three pH: 2.8, 6.3 and 10.0 (using phosphate buffer) and 1:5:1 ratios of phenol:H_2O_2:Fe(II) were conducted. At neutral or basic pH no reduction of the *p*-nitrophenol absorbance was observed in 500 s. Meanwhile, at pH = 2.8, a t1/2 of ca. 50 s is observed.

3. NaCl Fenton inhibition

In Figure 3 the influence of addition of NaCl to a reaction mixture 1:5:1, *p*-nitrophenol, H_2O_2, Fe(II) is shown in terms of percentage of *p*-nitrophenol transformation. For comparison, a reaction without NaCl is also shown.

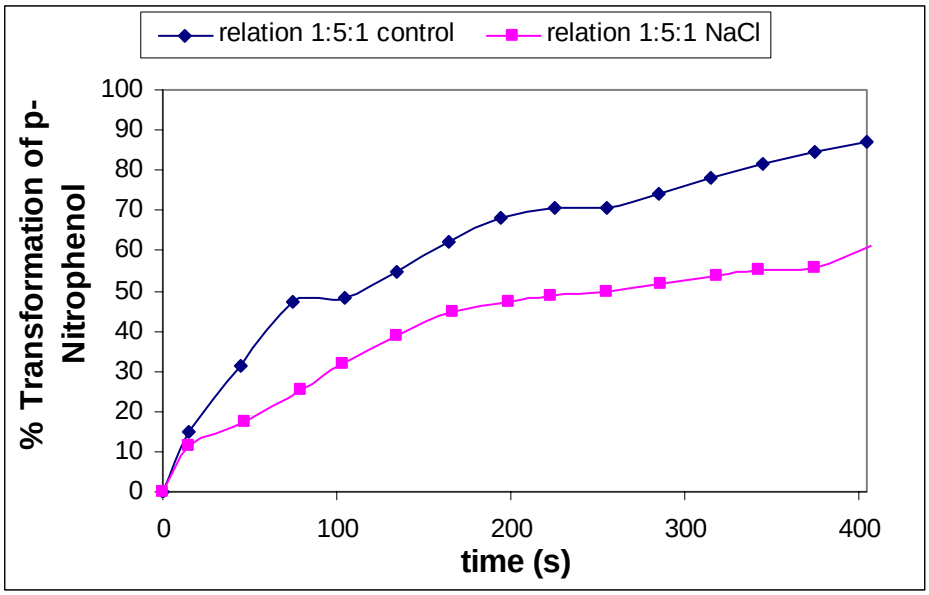

Figure 3. Fenton inhibition promoted by NaCl addition**. Bottom line:** Initial conditions: [*p*-Nitrophenol]=1,01(±0,03)x10^{-4} M,[H_2O_2]=5,0 (±0,2)x10^{-4} M, [Fe^{+2}]=1,00(±0,02)x10^{-4} M, [NaCl]=1x10^{-4}M, pH=2,8, λ=330nm). **Top line**: without NaCl. pH= 2.8, T= 25 ^{o}C.

According to the results, a ratio 1:5:1 (*p*-nitrophenol: H_2O_2: Fe(II)), pH ca. 3 and a minimum of salinity on the effluent to be treated are conditions that guarantee an efficient phenol degradation and mineralization. The rate limiting step is independent of the contaminant, therefore these conditions may also be used to degrade other contaminants.

The rate limiting step is indeed hydroxyl radical formation as it has been previously[11-14] recognized. However, in this study it has been found that a pre-equilibrium between free Fe(II) and H_2O_2 and a Fe(II)-$(H_2O_2)_n$ is established previous to the internal electron transfer that forms hydroxyl radical and Fe(III). This equilibrium is supported by the change in observed rate with [H_2O_2] and the observed salt effect where free species are stabilized compared to the aggregated complex. The hydroxyl radical oxidation of *p*-nitrophenol occurs in a fast step as supported by the zero order kinetic dependence on [*p*-nitrophenol][19]. The results also support the well recognized[13,18] cyclic character of Fenton reagent in which Fe(II) is regenerated from Fe(III) in a slow reaction through Fe(III)-H_2O_2 electron transfer.

4. Intermediates identification

p-Nitrophenol oxidation intermediates, using Fenton reagent, were identified by GC/MS using the procedure indicated in the experimental section. The identified intermediates were: *p*-nitrocatechol, hydroquinone and a dibenzofuran derivative (1,2,3,4,4a,9b-hexahydro-9-hydroxy-benzo(b)benzofuranol). In Figure 4, these intermediates are shown. Mass spectrum: m/z (rel.intensity %): *p*-nitrocatechol: 155[$M^{\cdot+}$](90), 139(40), 109(100), 80(60); hydroquinone:

110[$M^{\cdot+}$](100), 81(20), 53(15); dibenzofuran derivative: 190[$M^{\cdot+}$](100), 161(30), 147(70), 136(35), 123(25), 110(30), 77 (5), 51(5).

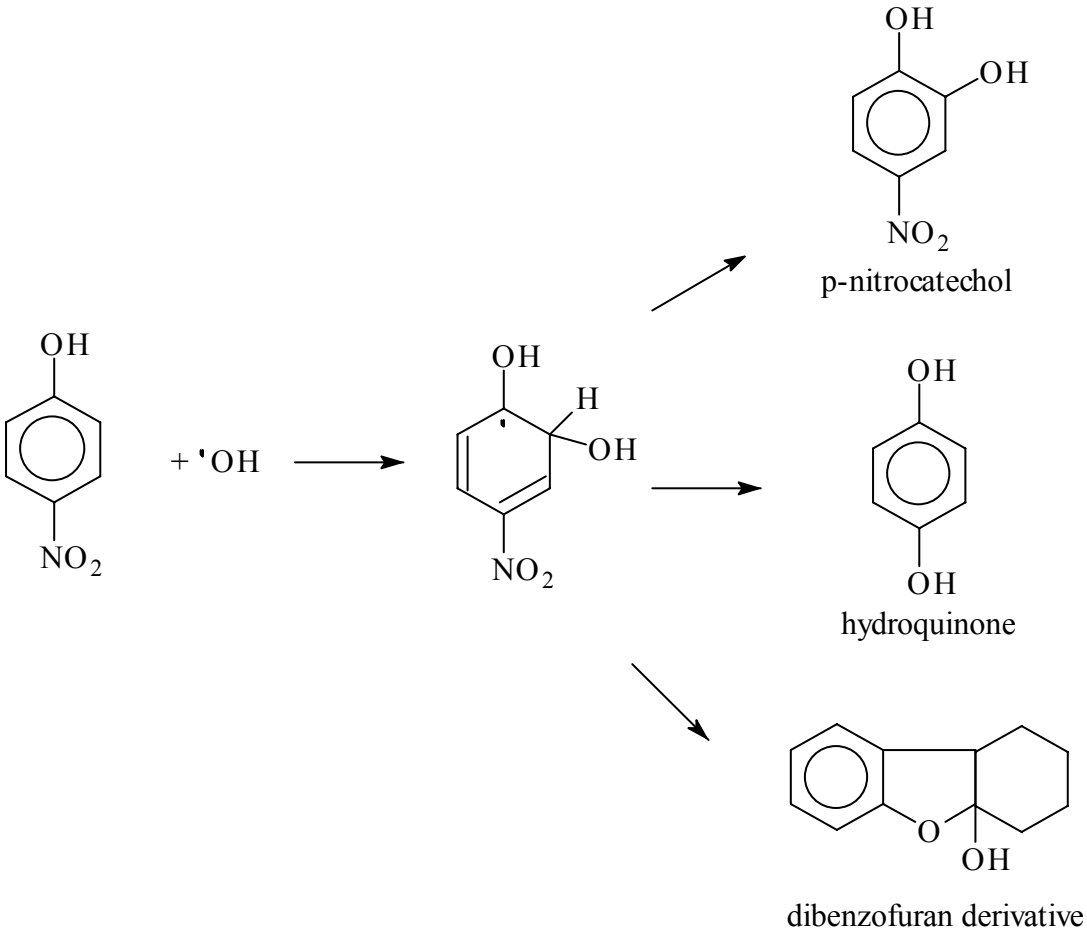

Figure 4. Hydroxyl radical degradation path for *p*-nitrophenol. The hydroxy *p*-nitrophenol radical (first step) has been previously proposed[7].

5. *p*-Nitrophenol mineralization

The rate of *p*-nitrophenol transformation in CO_2, H_2O and NO_2^- , was monitored by measuring COD (chemical oxygen demand). Using 1:5:1 and 1:8:1 (*p*-nitrophenol:H_2O_2:Fe(II)) ratios, COD decreased 50% (relative to the COD measurement after ca. 300 s) in 35s. This indicates that mineralization and degradation of *p*-nitrophenol proceed at equal rates. Therefore, the rate limiting step for mineralization is also that for hydroxyl radical formation.

6. [Fe(II)] and Fenton rate

Experiments varying [Fe(II)], show that the reaction suffers an inhibition when the [Fe(II)] > [*p*-nitrophenol]. The $OH^{\cdot}$ formed reacts with the excess of Fe(II) to produce Fe(III) and OH^{-}. This side reaction competes with the substrate hydroxyl radical consumption. This inhibition has been also observed[6] previously.

7. Oxalic acid Fenton complex

In Table 2, pseudo first-order rate constants obtained according to the procedure described in the experimental section, are shown. These rate constants correspond to different reaction conditions. As observed from the first two experiments, addition of oxalic acid produces appreciable increase in the k_{obs} value. We have interpreted this increase in rate as the result of a parallel participants mechanism: the traditional $OH^{\cdot}$ formation (Eq. 4) and a Fe(III) formation via oxalic acid complex. Since the rate constant of the first mechanism has been measured independently (second row data in Table 2), for the last mechanism, the observed rate is given by the difference of the two first k_{obs} values of Table 2. This k_{obs} corresponds then to the pseudo first-rate constant of the Fe(II)-oxalic acid reaction path. It is worth noting that when Fe(III) is used to form the oxalic acid complex (last data of Table 2), *p*-nitrophenol degrades (without an induction period) with a rate constant very similar to that of the Fe(II)-oxalic acid path. Therefore, we conclude that Fe(III)-oxalic acid complex is a common intermediate for the Fe-oxalic acid path no matter what the oxidation state of Fe. In Eq. 7, the Fe-oxalic acid path proposal is shown. It has been reported[20] that reaction shown in Eq. 6 proceeds rapidly.

Table 2. Pseudo first-order rate constants for the Fenton reagent reaction at different initial conditions. [1]Value obtained from Figure 2. [2]Value obtained from the difference of the two first values

Reactions in Acid Media pH = 2.8, T= 25 °C	k_{obs} (s^{-1})
Fe(II) + Oxalic Acid + H_2O_2 Molar relation (1:1:14)	3,3 (±0,2) x 10^{-2}
Fe(II) + H_2O_2 Molar Relation (1:14)	1.5 x 10^{-2} (1)
Fe(II)-Oxalic acid + H_2O_2	1.8 x 10^{-2} (2)
Fe(II) + Oxalic Acid + *p*-nitrophenol + H_2O_2 Molar Relation (1:1:1:14)	7,0 (±0,8) x 10^{-3}
Fe(III) + Oxalic Acid + *p*-nitrophenol + H_2O_2 Molar Relation (1:1:1:14)	6,7 (±0,5) x 10^{-3}

$$\text{Fe(II)} + \text{Oxalic acid} \overset{H_2O_2}{\rightleftharpoons} \text{Fe(II)-oxalic acid-}H_2O_2 \rightleftharpoons \text{Fe(III)-oxalic acid} + OH^- + OH^{\cdot} \quad (6)$$

$$\text{Fe(III)-oxalic acid} \overset{H_2O_2}{\rightleftharpoons} \text{Fe(III)-oxalic acid-}H_2O_2 \quad (7)$$

We have also followed the reaction potential to donate electrons through the measurement of COD (chemical oxygen demand). Under conditions in which Fe(II) or Fe(III) are mixed with an excess of H_2O_2, an important increase of COD occurs during the first 20 s of the reaction time. After that time, COD remains constant for more that 300 s. Formation of the oxalic acid–Fe complex itself does not produce COD increase, as it has been found in an additional experiment. It has also been reported[4] that Fenton reagent does not oxidize oxalic acid. Therefore, a new complex such as the one proposed in Eq. 7 must be formed. This Fe-oxalic acid-H_2O_2 complex may suffer internal electron transfer to produce an Fe(IV) radical species that increases COD via intermolecular electron transfer to an oxidant agent (O_2/H_2O). It has been reported[14,17] that the Fe(IV) species are unstable. For instance, it is not formed when Fe(III) is treated with H_2O_2. Instead of further Fe (III) oxidation, this species is reduced to yield Fe(II) and superoxide anion radical. However, when oxalic acid is added Fe(IV) could be formed due to an intramolecular delocalization of the electron coming from Fe. This delocalized Fe(IV) species represents a alternative path for oxidation in which the oxidant is this species instead of hydroxyl radical. Some experimental evidence supports the involvement of this alternative path: **1**.- When Fe(III), oxalic acid and H_2O_2 are mixed with *p*-nitrophenol, immediate degradation of the phenol is observed. Therefore, Fe(III) is not reduced to Fe(II) by H_2O_2 when oxalic acid is added to the reaction mixture. Otherwise, an induction period (such as the one obtained when Fe(III) and H_2O_2 are mixed) would have been observed. **2**.- When Fe(III), oxalic acid, H_2O_2 and *p*-nitrophenol are mixed, an increase of the COD of the mixture is observed after ca. 20-30 s. (Figure 5). **3**.- When Fe(II) or Fe(III) are mixed with oxalic acid and H_2O_2, an immediate (ca.30 s) increase in the COD is observed. All these results are in agreement with the reaction paths shown in Figure 6. In the Fe(III)-oxalic acid-H_2O_2 complex formed, an internal electron transfer occurs to form the Fe(IV) species that is stabilized by electron delocalization through the carboxylic group. As shown in Figure 6 (path **a**), an oxidizing agent such as O_2 could be consumed (increasing COD) accepting the delocalized electron to yield H_2O_2, 2 CO_2 (from oxalic acid) and Fe(III). The complex may also act as oxidant accepting an electron from *p*-nitrophenol to produce a radical cation that finally produces cathecol radical from where oxidation continues.

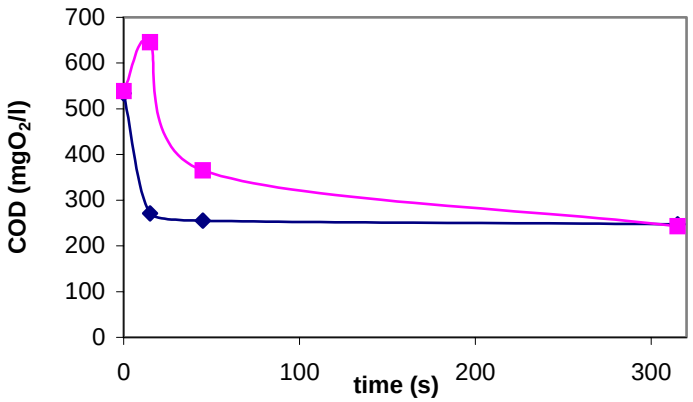

Figure 5. Chemical oxygen demand (COD) vs. time plot. **Top line**: Fe(III):oxalic acid: H_2O_2: *p*-nitrophenol (1:1:5:1) **Bottom line**: Fe(II):oxalic acid:H_2O_2: *p*-nitrophenol (1:1:5:1). T = 25°C. pH = 2.8.

As shown in Figure 5 , the initial (after ca. 20 s) COD increase is not observed in the case of Fe(II) when *p*-nitrophenol is added to the reaction mixture. This is probably due to the immediate consumption of *p*-nitrophenol via the hydroxyl radical that is produced before the Fe(III)-oxalic acid-H_2O_2 complex is formed. When *p*-nitrophenol is not added to the reaction mixture the increase in COD is observed no matter what the oxidation state of Fe. This is indeed an indication that even when Fe(II) is used, the Fe(III)/Fe(IV) complex (Figure 6) is formed. In fact, its contribution in terms of kobs value is comparable (as shown in Table 2) to the hydroxyl radical path.

Conclusions

In this work, we have found that the rate limiting step in the Fenton reagent reaction is the hydroxyl radical formation from a Fe(II)-$(H_2O_2)_n$ complex which is in equilibrium with the Fe(II) and H_2O_2 free species. For n > 10, no further increase in the k_{obs}. is obtained. The reaction is inhibited when NaCl is added due to the destabilization of the less solvated Fe(II) free species when compared to the aggregated form. The reaction is acid catalyzed in agreement with OH^- formation as one of the reaction products. When Fe(III) is used, instead of Fe(II) no reaction is observed during a period of 500 s. After that period, oxidation of *p*-nitrophenol, at pH = 2.8 occurs with kobs similar to the Fe(II), Fenton reagent one (2.3×10^{-2} s^{-1}). The observed induction period corresponds to the Fe(III) and H_2O_2 reaction to yield Fe(II) and the protonated form of the superoxide radical anion. When oxalic acid is added to the reaction mixture, an alternative oxidation path occurs with a kobs = 1.8×10^{-2} s^{-1}. This alternative pathway consists of Fe(III)-oxalic acid-H_2O_2 complex formation. An intramolecular electron transfer in the complex is proposed in order to explain the immediate reaction when Fe(III) is used instead of Fe(II) and the

initial increase of COD (chemical oxygen demand) when *p*-nitrophenol is absent or in its presence when Fe(III) is used.

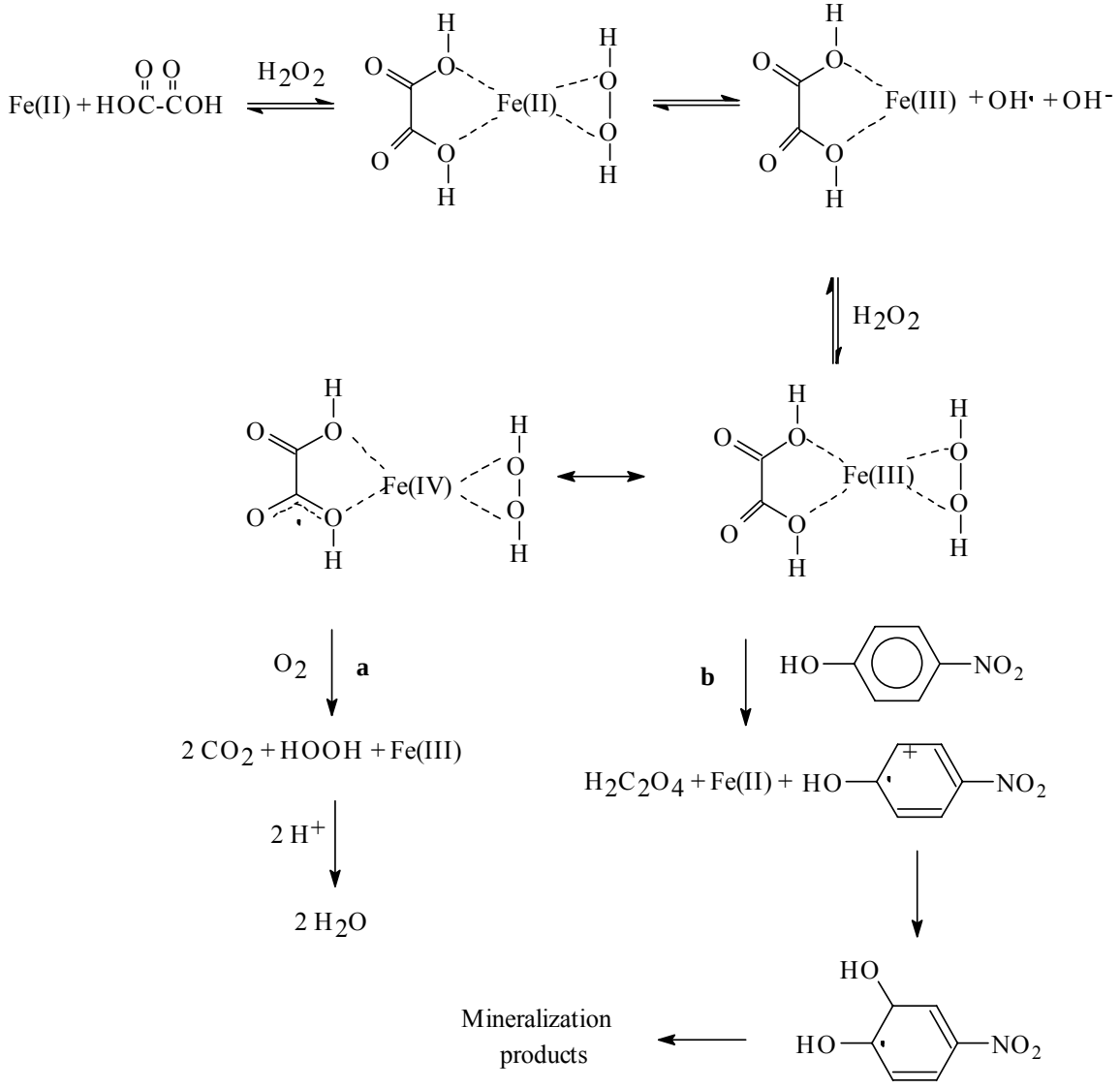

Figure 6. Fenton reagent reaction in presence of oxalic acid. Fe(III)-oxalic acid-H_2O_2 is the key intermediate. Path **a** explains the observed initial increment of COD. Path **b** illustrates the oxidizing properties of the complex.

Experimental Section

Fenton experiments

Fresh, $FeSO_4.7H_2O$ (from Scharlau) solutions were prepared before kinetics runs. pH was adjusted with H_2SO_4 0.1 M solution. UV-visible (Hewlett Packard, model 8452 A, diode array) was used to monitored reaction progress by following either the Fe (III) band at 220 nm or the *p*-nitrophenol degradation at 330 nm. In experiments without adding *p*-nitrophenol, H_2O_2 (from Riedel de Haén, 35%) was added to the Fe (II) solution previously prepared in a UV quartz cell. Added volumes were taken into account to the reactants final concentrations. Reaction was monitored each 8 s during the first 8 min and each 60 s during the following 30 min. Triplicates of each experiment were used to evaluate the mean and standard deviation of the rate constants. Rate constants were obtained from the slope of ln ($A_{inf.}$-At) vs. t plots (A; absorbance). In reactions in which *p*-nitrophenol was included, solution were prepared in the UV quartz cell together with the Fe (II) solution. To the mixture, H_2O_2 solution was added and the reaction was monitored by following *p*-nitrophenol absortion band (330 nm). 1:1:1 (phenol:H_2O_2:Fe(II)) and 1:5:1 molar ratios were used. Reactions were monitored each 30 s during the first 12 min and each 60 s for additional 12 min. Rate constants were obtained from plots of ln [phenol] vs. t. Previously, A (absorbance) vs. [phenol] calibration curves were obtained. Reactions with Fe(III) ($Fe_2(SO_4)_3.xH_2O$), from Riedel de Haén) were conducted using the same experimental conditions as when Fe(II) was used. The reaction was quenched by adding methanol (98%, from Riedel de Haén). Reactions with oxalic acid were conducted using the following Fe:oxalic acid: H_2O_2 ratios: 1:1:14 and when phenol was included, phenol:H_2O_2:Fe:oxalic acid: 1:5:1:1.

In order to optimize reaction conditions, experiments varying [H_2O_2] at the following phenol (1.2×10^{-2} M):H_2O_2:Fe(II) ratios, were performed: 1:0:1, 1:5:1, 1:8:1, 1:11:1, 1:14:1, 1:17:1 and 1:20:1. [Fe(II)] was also varied according to the following ratios: 1:14:0, 1:14:0.25, 1:14:0.5, 1:14:0.75, 1:14:1 and 1:14:1.5. A ratio of 1:5:1, [NaCl]: 1.0×10^{-4} M was used and pH (2.8, 6.28 and 10, adjusted with phosphate buffer) at reactants ratio:1:5:1 were used to conduct experiments.

Reaction intermediates identification

p-Nitrophenol reaction intermediates identification at the reaction ratio: phenol (1.2×10^{-2} M):H_2O_2: Fe(II): 1:0:1, 1:0.5:1,1:1:1, 1:2:1 and 1:5:1 was made as followed: 15 s after reaction initiation, 0.5 ml of methanol was added. Extraction was carried out with dichloromethane (HPLC grade 99.8% from Merck). The organic layer was dried with anhydrous sodium sulfate and the solvent evaporated by means of Tymark turbo vap II solvent concentrator at 25 ^oC. 5 uL extracts were injected (300 ^oC) into a GC/MS Hewlett Packard chromatograph model HP 6890 provided with a mass detector model HP 5973. Helium was used as carrier at 1ml/min. A 30 m x 0.25 mm DB-5625 column was used with the following temperature arrangement: 10 min at 135 ^oC, 20 ^oC/min until reach 280 ^oC and additional 5 min at that temperature. Mass detector was operated in scan mode (28-300 mau) in selective ion monitoring mode at 70 ev.

Mineralization experiments

Mineralization experiments were run under identical conditions to degradation experiments. However, the reaction was monitored measuring COD (chemical oxygen demand) using an

HACH colorimetric method: 2 ml of sample is digested with HACH $K_2Cr_2O_7$ solution at 150 ^oC for 2 h. The Cr(III) formed is followed at 620 nm using a HACH DR/2010 spectrophotometer.

Acknowledgements

We acknowledge UGA-USB, INTEVEP and CONIPET (project: 97-003767), for the financial support.

References and Notes

1. Fenton, H.J.H. *J. Chem. Soc.* **1894**, *65*, 899.
2. López, R.; Núñez, O.; Morales, F.; Calderón, C.; Liewald, W. *Acta Científica Venezolana* **1999**, 50, 1, 75.
3. Safarzadeh-Amiri, A.; Bolton, J.; Cater, S. *J. Adv. Oxid. Technol.* **1996**, 1,1,18.
4. Bigda, R. *Chem. Eng. Prog.* **1995**, 62.
5. Rahhal, S.; Richter, H. *J. Am. Chem. Soc*. **1988**, *110*, 3126.
6. Ma, Y.; Huang, S.; Lin, J. *Water Science & Technology* **2000**, *42*, 3-4, 1155.
7. Oturan, M.; Peiroten, J. ; Chartrin P.; Acher, A. *Environ. Sci. Technol.* **2000**, *34*, 3474.
8. Sedlak, D.; Andren A. *Environ. Sci. Technol.* **1991**, *25*, 4, 777.
9. Barbeni, M.; Minero, C.; Pelizzetti, E. *Chemosphere* **1987**, *16*, 2225.
10. Tyre, B.; Watts, R. ; Miller, G. *J. Environ. Qual.* **1991**, *20*, 832.
11. Merz, J.H.; Waters W.A. *Discuss. Faraday Soc*. **1947**, *2*, 179.
12. Haber F.; Weiss J.J. *Proc. Roy. Soc. London*, Ser. A. **1934**, *147*, 332.
13. Walling, C. *Acc. Chem. Res*. **1975**, *8*, 125.
14. Walling, C.; Amarnath, K. *J. Am. Chem. Soc*. **1982**, *104*, 1185.
15. Yamazaki, I.; Piette, L. *J. Biochem. Chem*. **1990**, *265*, 23, 13589.
16. Groves, J.T.; Vander Puy. M. *J. Am. Chem. Soc*. **1976**, *98*, 5290.
17. Groves, J.T.; Nemo T.E.; Meyer, R.S. *J. Am. Chem. Soc*. **1979**, *101*, 1032.
18. Walling, C.; Goosen, A. *J. Am. Chem. Soc*. **1973**, *95*, 9987.
19. The kobs. is independent on [*p*-nitrophenol]; however, a plot of ln [*p*-nitrophenol] vs. t corresponds to a typical pseudo first-order plot since the radical, that is consumed rapidly by *p*-nitrophenol, is produced in the rate limiting step under first order conditions.
20. Zuo, Y.Y.; Hoigné, J. *Environ. Sci. Technol*. **1992**, 26, 5, 1014.